Experimental investigation of a full-scale masonry cross vault subjected to vertical settlement

Benjamin Torres, Elisa Bertolesi*, Juan J. Moragues, Pedro A. Calderón, Jose M. Adam

ICITECH, Universitat Politècnica de València. Camino de Vera s/n, 46022 Valencia, Spain

Abstract

Masonry cross vaults are among the most beautiful structures ever created by the human race. Although cross vaults have been the subject of diverse numerical and experimental studies, they are still in need of further study, for example, the effect on their behaviour of the differential settlement of their supports. However, of all the experiments carried out on these structures so far none has been on full-scale specimens. In the study described here, carried out at the ICITECH laboratories of the Universitat Politècnica de València (Spain), a full-scale timbrel cross vault was constructed and tested under the vertical settlement of one of its supports. The design of the vault resembled those in a church on the outskirts of Valencia, one of which had collapsed due to the settlement of its supports. Thanks to the ambitious monitoring system used, the behaviour of the vault could be characterised from the results obtained in the tests.

Keywords: Cross vault; Brick; Masonry; Settlement; Full-scale; Experiment

* Corresponding author. Tel.: +39 3496597648.

E-mail address: elber4@upv.es (E. Bertolesi).

1. Introduction

Most historical constructions are made of masonry. Mortar joints and solid blocks generally compose this material, which can be considered a heterogeneous material. During the centuries and depending from the local availability of the row materials, masonry has been constructed using different kind of blocks and type of mortars. As expected, its variety makes assessing a masonry building's safety particularly challenging, from both a numerical and experimental point of view. In spite of this, masonry material often exhibits an orthotropic behaviour characterized by a negligible tensile strength and experiences far lower compressive stresses than its actual capacity [1]. Therefore, it might exhibits some peculiar cracking phenomena, which comprised: (i) sliding in mortar joints, (ii) tensile cracking in the blocks, (iii) diagonal tensile cracking in blocks and (iv) frictional behavior of the joints. In addition, although most of the masonry constructions being part of the architectural heritage have been constructed following rules of thumb, they are currently subjected to different types of loads, for example: overloading, dynamic actions, settlement, in-plane and out-of-plane deformations [2–4], which can worst their behaviour or even led to their collapse. Some dramatic examples of these events have occurred throughout history and even more recently [5,6]. They show the importance of improving our knowledge of masonry structures. In particular, the damage suffered by many historical churches and buildings after the recent Italian earthquakes [6–10] has shown that masonry vaulted structures are particularly vulnerable to seismic action.

In addition to dynamic vibration, the heaviest loads on these structures are foundation settlement and seasonal temperature changes [11]. Differential settlements in the support have adverse effects on the serviceability and stability of vaulted masonry structures, may result in deformations, cracking, and cause changes in their geometry,

54 twist and vertical alignment [12–14]. Evaluating the consequences associated with
55 foundation or support movements, both in terms of damage (i.e. crack width) and
56 collapse (i.e. amount of support displacements involving loss of stability), is one of the
57 main questions that has attracted the attention of the architects and engineers who have
58 to assess historical and other types of masonry constructions.
59 Some of the most extreme examples that posed significant challenges to builders were
60 the differential foundation settlements of Venetian masonry buildings caused by soft
61 soils [15], the settlement mechanisms in the naves of the Cathedral of Milan due to
62 subsidence [16] and in the Cathedral of Agrigento due to slope instability problems
63 [17], to cite just a few. As can be noted in the cited examples, a large part of the
64 architectural heritage comprised masonry vaulting systems. Indeed, cross vaults have
65 played a very important role in the history of architecture. For example, tile vaults left
66 their mark not only on Spanish and colonial architecture, but many Spanish architects
67 and master builders, e.g. Guastavino, used this type of structure extensively in America
68 in the 19^{th} and 20^{th} centuries. In order to study the behaviour of a masonry cross vault
69 subjected to vertical settlement in one of its supports, numerical models and
70 experimental tests have been performed in recent years. The numerical modelling of
71 masonry structures demands a knowledge of different masonry mechanical parameters
72 such as its elastic behaviour, the compression, tensile and shear strengths of stone
73 materials and mortars, friction angles and cracking energies [18–20]. Due to the
74 difficulty of characterising the properties of masonry and its three-dimensional
75 behaviour, laboratory and *in situ* testing are vital. To this scope, laboratory
76 investigations on small scale specimens might help to characterize the mechanical
77 behaviour of the constituent materials, whereas experimental campaign on in-situ full
78 scale specimens are useful to understand the actual structural behaviour of complex

structures when subjected to a variety of excitations. As expected, this latter type of investigation is more expensive and more difficult to be performed than the previous one and therefore it has been carried out only on few replicates. As a matter of fact, some tests on masonry structures have been reported in the literature, and few of the tests carried out to date have been on full scale specimens. For this reason, full-scale tests are needed in order to fully characterise the three-dimensional behaviour of masonry cross vaults, especially in vaults under the vertical displacements of a support, which has never been studied before.

De Lorenzis et al. [21] tested a ½ scale semicircular vault subjected to a distributed gravity load. Theodossopoulos et al. [22], Mazarredo Aznar [23], Theodossopoulos et al. [22] tested a wooden cross vault pointed arch, subjected to its own weight and horizontal movements of the supports. Mazarredo Aznar [23] tested an elliptical section tile groin vault under a gravity load. Considering the limited amount of research that has been done in this field, the aim of the present study is to investigate the behaviour of cross vaults subjected to vertical settlement in one of their supports. This paper therefore describes the experimental test carried out on a full-scale timbrel cross vault subjected to differential settlement in one support.

2. Definition of experimental test

The laboratory investigation comprised the test of a full-scale timbrel masonry cross vault subjected to a monotonically increased vertical displacement in one of its support to simulate soil settlement. The experimental campaign has been aimed at assessing the structural behaviour of masonry vaults during this type of event using the data collected by traditional (i.e. Linear Variable Displacement Transducer sensors) and innovative (i.e. Fiber Optic sensors) sensors located along the whole surface of the vault. The monitoring strategy adopted has been intended to detect the activation of different

collapse mechanisms which might led to its partial or total failure. To assess the potentialities of the proposed network of sensors, a masonry vault has been constructed at the ICITECH laboratories of the *Universitat Politècnica de València* (Spain) using as reference the vaults in the San Lorenzo parish church in Castell de Cabres, Spain (Figure 1-a). It is important to note that, the church experienced a series of soil settlement-induced damages, which caused one of the vaults to partially fail and multiple cracks in the others.

2.1. Geometry and experimental set-up

As indicated previously, the geometry of the tested vault has been defined in accordance with those in the Parish Church of San Lorenzo (Figure 1-a), with slight modifications to adapt to laboratory conditions.

Figure 1. Plan view of the Parish Church of San Lorenzo [34] and partial collapse of a vault over the choir.

This church, built in 1750, contains timbrel cross vaults in the side naves and over the baptistery [24].The cross vaults in this church are composed of two layers of bricks with a total thickness approximately equal to 80 mm (Figure 1-b). As can be noted in Figure 1-b, the masonry vault constructed in the ICITECH has been characterized by four 3.6 m lateral semi-circular section arches built on formwork. The arches were 160 mm thick and consisted of four layers of bricks, joined by gypsum plaster (first and third layers), cement mortar (second layer) and lime mortar (fourth layer). The first layer was used as formwork for the further layers, thanks to the quick-drying gypsum plaster. The

webbing had two layers of bricks cemented by a gypsum plaster paste for the first layer and lime mortar for the second. In addition, the second layer of bricks has been laid perpendicularly to the first. Finally, it is worth mentioning that the vault has been conducted following the traditional method used to build Spanish timbrel vaults.

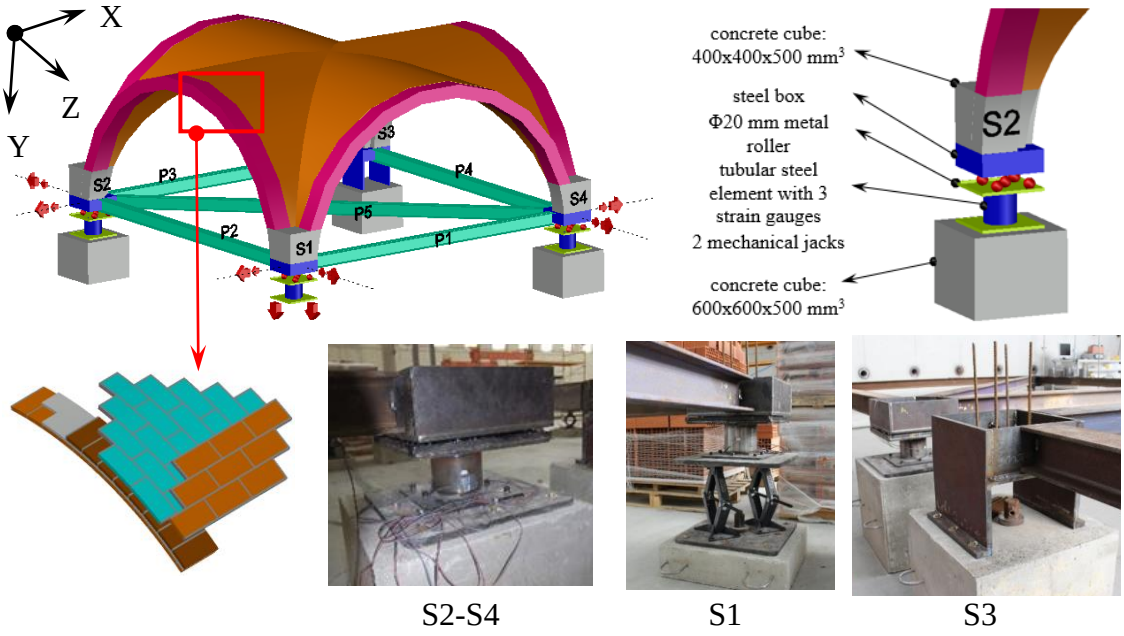

Figure 2. Experimental set-up adopted during the test.

The vaults rested on four supports (S1, S2, S3 and S4), formed of steel elements, designed to allow monitoring of vertical reactions during construction and testing. Support S1 (Figure 2) was formed by a steel box supported on 20 mm diameter metal rollers, allowing free movement in both horizontal directions. Below the rollers there was a 159 mm diameter, 200 mm high and 2 mm thick tubular steel element to allow monitoring the reactions by means of three strain gauges. In its turn, this element rested on a 20 mm thick metal plate firmly joined to two mechanical jacks which applied the vertical displacements. The jacks were anchored to a 600x600x150 mm^3 concrete block, with a 60 mm orifice at its centre, through which the entire support has been fixed to the laboratory reaction floor slab. Conversely to support S1, supports S2 and S4 have been restrained with respect to vertical movements, whereas horizontal displacements were possible. To this scope, the 20 mm metal plate supporting the tubular element has been

directly anchored to a 600x600x520 mm^3 concrete block. Finally, S3 has been directly anchored to a 600x600x500 mm^3 concrete block (Figure 2). A detailed sketch of the parts forming support S2 has been depicted in Figure 2. A solid concrete structure rested on each of the supports forming a square 4 m long base for the four arches (Figure 2). In order to prevent the activation of a failure mechanism produced by the free horizontal movements of supports S2 and S4, and simulated the presence of contiguous vaulting systems, a lattice frame of steel girders (Figure 2) has been used. To this scope, five steel beams (with height equal to 140 mm) have been hinged to the steel boxes supporting the masonry vault. A detail of the connection used is showed in Figure 2, where it can be noted that the welded surface has been reduced to the central portion of the beam to prevent the transmission of bending moments and allow axial movements only.

2.3. Material properties

This section is aimed at describing the laboratory tests performed to characterize the mechanical properties of the materials adopted during the construction of the vault. Solid clay bricks with dimensions equal to 230×110×26 mm^3 and a specific weight of 1820 kg/m^3 have been used to construct the whole vault. The bricks have been tested in simple compression and with three points bending test, as showed in Table 1. Furthermore, in Table 1 have been listed the results obtained at the end of the experimental tests.

Table 1. Laboratory tests performed to characterize clay bricks.

	N. of specimens [-]	**Dimensions**	**Elastic Modulus [MPa]**	**Strength [MPa]**
Compression test	8	47x26x26 mm^3	4333	47.6
Three points bending test	3	Full bricks: 230x110x26 mm^3	-	11.1

Similarly to the clay bricks, the three types of mortars have been characterized by means of a series of laboratory tests. The lime mortar contained natural pozzolan and has been provided by the GRUPO PUMA [25]. The cement employed has been identified as I-42.5 MPa. The dosages in kilos of all the materials used to build the vault have been summarized in Table 2. The bending and compressive strengths of gypsum plaster and mortars used to lay the bricks have been assessed at different ages, in accordance with the current standards [26]. A total of 18 bending and 36 compression tests have been carried out on the different materials. A summary of the strengths can be seen in Table 3.

Table 2. Dosage of cement mortar, lime mortar, gypsum plaster and concrete.

Kg	Cement	Sand	Gravel	Water	Lime	Gypsum Plaster
Cement Mortar	5	25	-	3.6	-	-
Lime Mortar	-	-	-	3.5	25	-
Gypsum Plaster	-	-	-	3	-	18
Concrete	190	470	450	90	-	-

Further experimental tests have been conducted to characterize the mechanical properties of the masonry constituting the vault web. A total of 10 specimens (four for compression and six for bending tests) have been employed to characterise the masonry assemblage. It is worth mentioning that, the brick distribution adopted is similar to that used in the webbing of the actual vault under study as visible in Figure 3, which shows the three points bending test carried out.

Table 3. Mechanical properties of constituent materials.

Type of mortar	Age [days]	Compressive strength [MPa]	Flexural strength [MPa]
Cement mortar	7	15.5	2.8
	28	16.1	3.6
Lime Mortar	60	9.4	2.1
Gypsum Plaster	7	7.22	2.4

The compressive strength of the specimens was between 8-10 MPa. The bending strength was more varied; four of the six specimens reached a value of 1.5 MPa while the other two reached 2,0 and 2.5 MPa.

(a) (b)

Figure 3. Three points bending test (-a) and failure mechanism (-b).

2.2. Preliminary numerical analysis

In order to properly design the experimental investigation at hand, the authors developed a linear elastic 3D finite element model by means of the LUSAS software [27]. To speed up the calculations and obtain a preliminary evaluation of the vault behaviour, the structure has been modelled by means of bi-dimensional FEs. The geometry of the vault has been obtained starting from the free span of the lateral arches, which resulted equal to 3.6 m. The obtained surface represents the mid plane of the webs vault.

Table 4. Elastic properties adopted in the FE model.

Material	**Density [kN/m^3]**	**Elastic Modulus [MPa]**	**Poisson ratio [-]**
Masonry	18	2100	0.2
Concrete	20	30000	0.2
Steel	78	209000	0.3

In detail, both webbing and arches have been simulated by shell-type elements, whereas the concrete structure over the support has been modelled by hexahedral elements. Finally, the steel beams have been simulated by two-nodes truss FEs. The analysis has been carried out under displacement control applying the following boundary

conditions. In detail, S3 has been clamped, S2 and S4 have been simply supported along the vertical direction only. Similarly, S1 has been not restrained along the horizontal plane, a vertical displacement has been applied to simulate a downward soil settlement. The vault has been subjected to two types of loads: 1) the self-weight and 2) a downward vertical displacement applied to S1. A summary of the density and the Elastic Moduli adopted for the constitutive materials has been provided in Table 4.It is worth mentioning that, the parameters adopted have been assumed according to the results of the laboratory tests developed to characterize the materials involved into the vault construction. The parameters of the concrete used for the support have been obtained from the results of practical tests on specimens, and the parameters for the steel were considered to be as provided by the manufacturer's specifications.

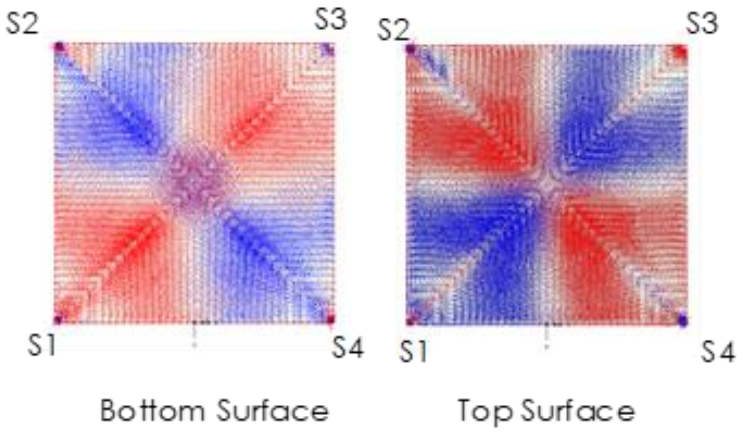

Figure 4. Principal stress maps obtained with an imposed displacement equal to 30 mm.

As clearly visible in Figure 4, the model has been able to identify the points in the vault that suffered the greatest stresses and thus where cracks could be expected to appear. In details, the critical points on the inner surface of the vault are concentrated along the elliptical arch that joins supports S1 and S3 and close to the support, while on the outer surface the stresses reached the maximum value in correspondence of the keystone of the elliptical arch joining supports S2 and S4. In both cases the tensile forces extend

towards the circular arches joining the supports. On the basis of the results obtained, it has been also possible to define the position of the sensors employed. In addition, the tensile forces acting in the truss FEs used to model the bracing frame has been used to design the steel profiles to be used during the experimental test.

2.4. Loading protocol and monitoring system adopted

As discussed previously, the proposed masonry vault has been tested applying a vertical downward displacement in support S1. In detail, the vertical settlement has been imposed by means of two mechanical jacks placed parallel to each other under the steel box visible in Figure 2. The downward displacement has been imposed manually in a quasi-static fashion synchronising the mechanical jacks to prevent any rotation of the support. The history of displacements applied is depicted in Figure 5. In addition, a total of 23 sensors have been placed along both the inner and outer surfaces of the structure to allow the monitoring of the vault behaviour. In detail, from the network of sensors employed during the test, it has been possible to extract information about: i) the reactions forces in correspondence of the supports, ii) the collapse mechanism with the widening of tensile and flexural cracks, iii) the horizontal displacements in the supports, and iv) the axial forces in the steel girders.

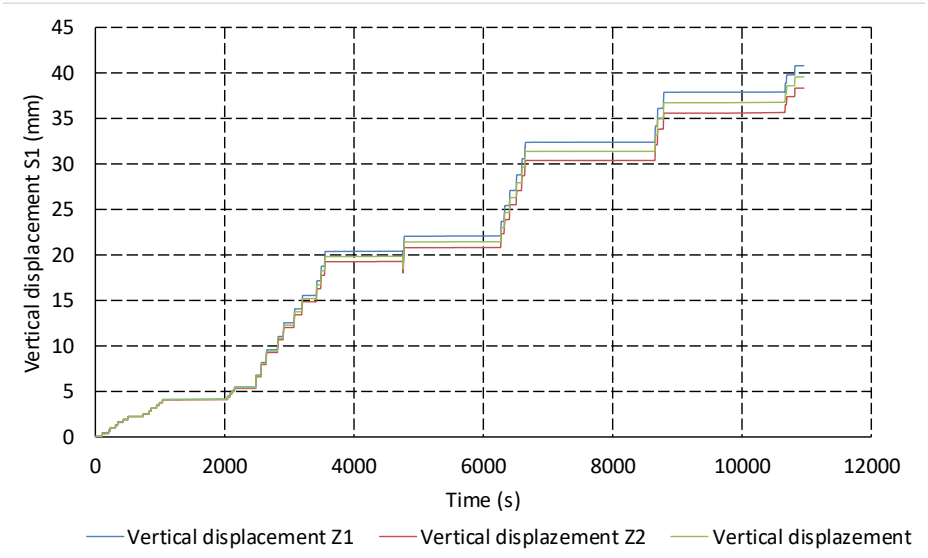

Figure 5. History of displacements applied to support S1.

The vertical reactions have been calculated starting from the average deformation of 3 strain gauges glued to each of the tubular steel element positioned in supports S1, S2 and S4. To eliminate the temperature effect, a control tube fitted with a strain gauge was kept in the laboratory and not subjected to loading. Displacements have been monitored at critical points by two types of long gauge sensors: 1) *Linear Variable Displacement Transducers* (LVDT), and 2) FBG-based long gauge fibre optic sensors [28,29]. Table 5 shows the sensors used and their positions, whereas Figure 6 depicts the positions of all the sensors employed in the proposed experimental campaign. In particular, sensors LVDT_Y1 and LVDT_Y2 have been installed on support S1 to measure settlement during the test (Figure 6-b). Sensors S1_X, S1_Y, S2_X, S2_Y, S4_X and S4_Y have been attached as shown in Figure 6-d on supports S1, S2 and S4. In addition, the loads on the steel girders used to join the supports have been monitored by means of strain gauges attached to the mid-point of the web plate.

Table 5. Long gauge sensors installed on the cross vault.

Type of sensor	**Length [cm]**	**Location**
LVDT1	60	On support S1, in elliptical arch S1-S3
LVDT2	39	On support S1, in elliptical arch S1-S3
LVDT3	59	On support S1, in elliptical arch S1-S3
LVDT4	64.5	On support S1, in elliptical arch S1-S3
LVDT5	45	On support S1, elliptical arch S1-S3
LVDT6	35	Upper surface of the vault, in elliptical arch S2-S4
LVDT7	36	Upper surface of the vault, in elliptical arch S2-S4
FOS1	32	On support S1, in elliptical arch S1-S3
FOS2	32	Upper surface of the vault, in elliptical arch S2-S4
FOS3	100	Upper surface of the vault, in elliptical arch S2-S4
S1_X	15	On support S1, horizontally in X direction
S1_Z	15	On support S1, horizontally in Z direction
S2_X	15	On support S2, horizontally in X direction
S2_Z	15	On support S2, horizontally in Z direction
S4_X	15	On support S4, horizontally in X direction

S4_Z	15	On support S4, horizontally in Z direction
LVDT_Y1, LVDT_Y2	30	On support S1, vertically in Y direction

The treatment of all the data recorded from the strain gauges and LVDTs has been performed on HBM CATMAN software [30], whereas the MicronOptics MOI ENLIGTH software has been used for the data from the fibre optic sensors [31].

3. Vault construction

In the first stage of building the vault, the four arches have been built on metal formwork. The first layer of bricks formed has been used as formwork for the following ones, as showed in Figure 7. The formwork has been removed after 48 hours.

The first part of the webbing has been laid in the corners between two arches. When the first layer reached an height about 1.5 m from the base of the arches, the second layer has been constructed perpendicular to the first. The whole construction process of the vault can be seen in Figure 7.

-a

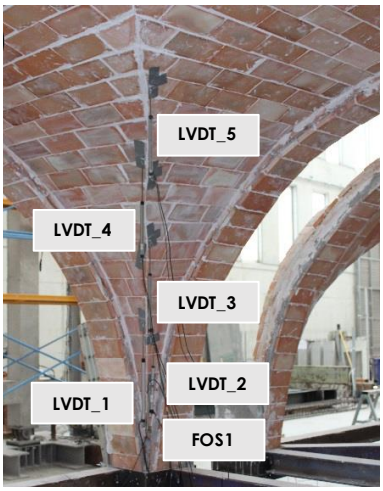

-b

-c 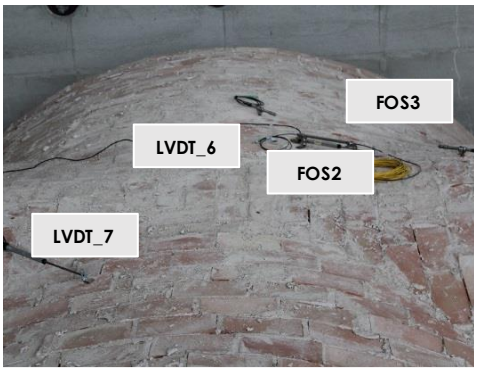

-d 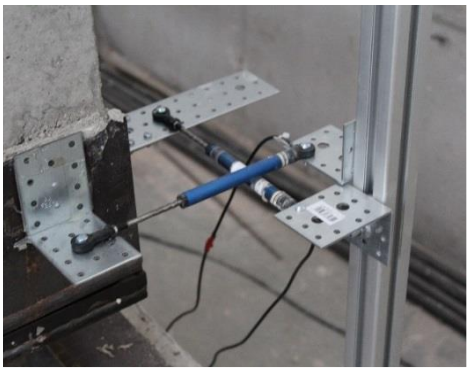

Figure 6. Position of long gauge sensors: along the elliptic arch S1-S3 (-a), in support S1 (-b), along the outer surface of the vault (-c) and in support S1, S2 and S4 (-d).

255

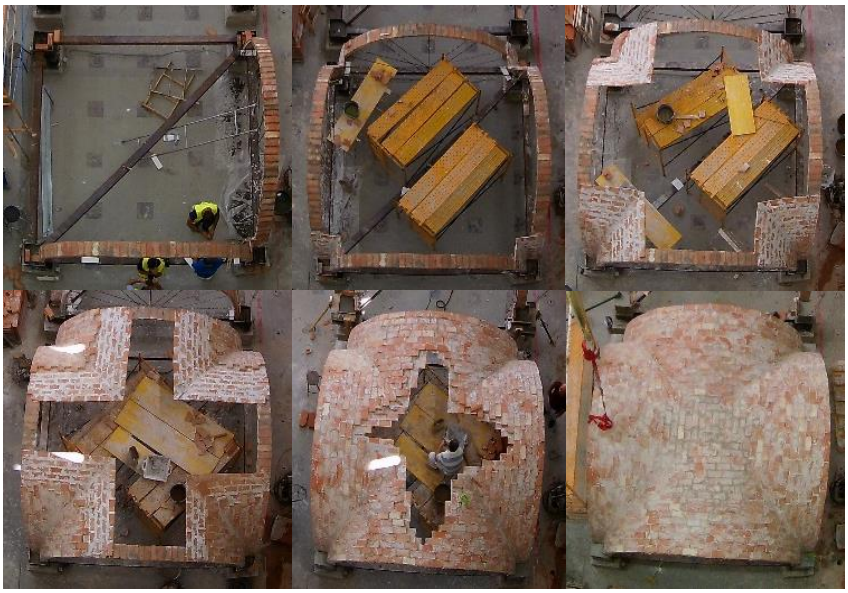

Figure 7. Construction phases of the vault.

256 ## 5. Analysis of results

257 This section contains a detailed analysis of the results obtained at the end of the
258 experimental campaign at hand. In detail, the laboratory outcomes have been subdivided
259 into: (i) vertical reactions calculated in supports S1, S2 and S4; (ii) development of
260 cracks and cracking mechanism of the cross vault and finally, (iii) the structural
261 behaviour of the masonry vault.

262

263 ### *5.1. Vertical reactions*

264 Figure 8-a shows the evolution of the reactions in the supports according to the
265 settlement applied in S1. The maximum settlement value applied to S1 was 40 mm. In

S2 and S4 the reactions rose while in S1 and S3 they diminished as settlement increased. In detail, S1 and S3 reactions fell in the order of 28% and 55% of their initial values, respectively, while those of S2 and S4 rose by 27% and 50%, respectively.

The reaction pairs S1-S2 and S3-S4 had similar evolutions; in the initial phase the evolution of the reactions is practically linear but becomes increasingly non-linear as settlement of S1 advances. As a matter of fact, the reactions were found to be linearly in proportion to the settlement value until this reached 5 mm. Between 5 and 10 mm they became non-linear and after 10 mm settlement the reactions remained practically constant or were even found to fall until the end of the test, in spite of the fact that S1 continued to settle. This behaviour was due to the appearance of the first cracks close to the supports, which re-distributed the loads over the rest of the webbing. Similarly, the loads on the girders that join the supports experienced the same evolutions (Figure 8-a and-b). In detail, P1, P2, P3 and P4 have been loaded with compressive forces, as clearly visible comparing Figure 8–b, whereas tensile forces higher than the compressive forces have been detected in P5. The loads on the girders increased with settlement up to 15 mm, after that point they remained relatively constant or even decreased slightly.

-a

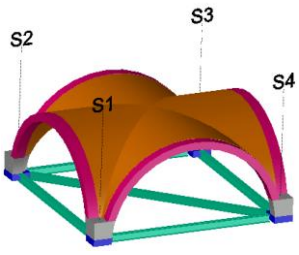

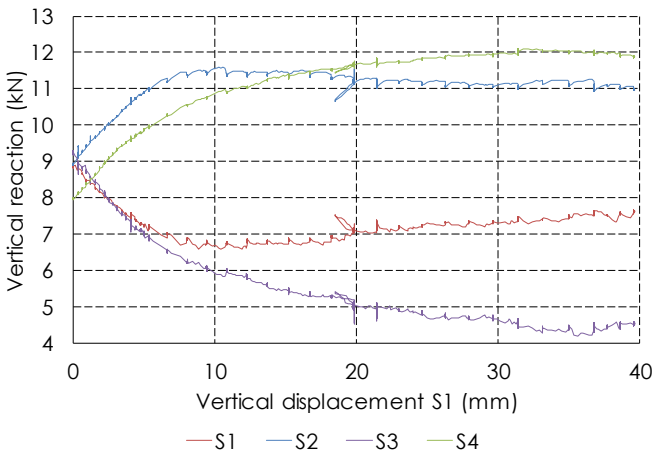

-b

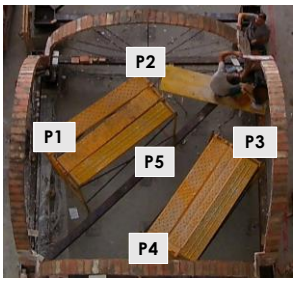

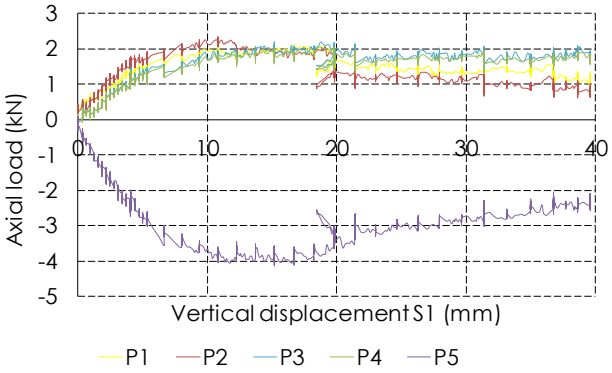

Figure 8. Evolution of reactions according to settlement of S1 (-a) and on the base bracing girders (-b).

5.2. Development of cracks

Figure 9 depicts the displacements recorded by means of the long gauge sensors, LVDTs and FOS, placed along the vault. It is worth mentioning that, all the sensors depicted in Figure 9 show displacements related to tensile stresses. Those installed on S1 along the S1-S3 elliptical arch (LVDT1, FOS1, LVDT2, LVDT3, LVDT4) show maximum displacements of 0.05 mm, while those attached to the cornerstone on the upper surface of the vault (LVDT6, LVDT7, FOS2 and FOS3), give considerably higher displacements of between 2 and 2.5 mm, indicating the presence of cracks. The value registered by LVDT5 on the lower vault face over arch S1-S3 reached 1 mm at the end of the test, indicating cracks in this area also.

-a

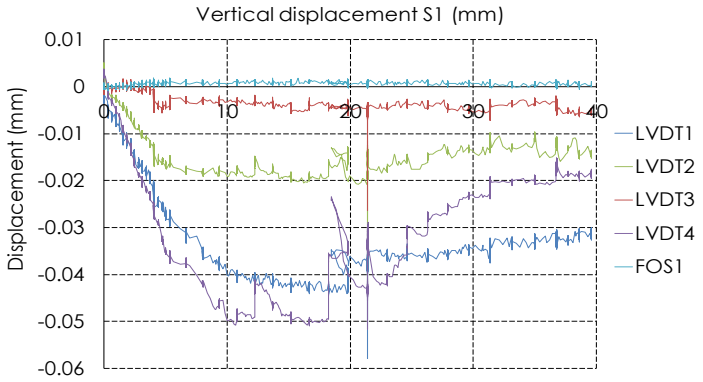

-b

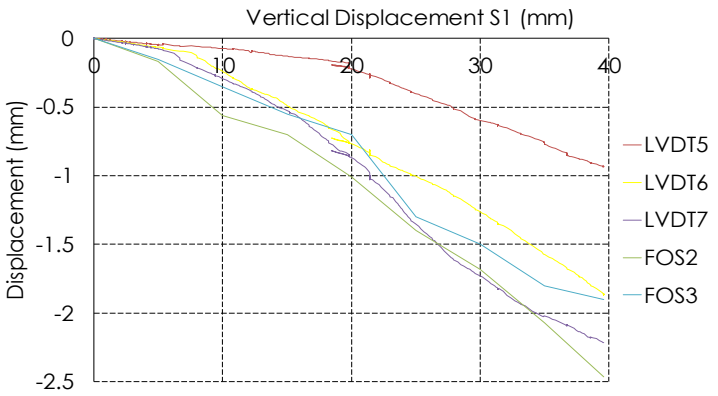

Figure 9. Displacements recorded by long gauge sensors.

293

294 The visual inspections carried out during and after the test revealed the zones where
295 cracks appeared. In general, two types of cracks have been detected: 1) those close to
296 supports and arches, and 2) those that developed on the vault masonry web.

297 The cracks close to S1 were tensile cracks caused by the settling of the support. These
298 started in the base of S1 towards S2 and propagated horizontally towards the S1-S3
299 elliptical arch following the inter-brick joints (Figure 10-a). However, those that
300 appeared in S2 have been caused by the bending of arch S2-S4 and also started in the
301 outer faces of the arches rising from S2. They have been propagated not only along the
302 joints but also through breaks in the bricks themselves. Since these were bending
303 cracks, their openings were wider on the outer face of the vault, where they reached a
304 maximum of 3 mm. Those on the inner face were narrower and shorter (Figure 10-b).
305 During the visual inspection carried out when the settlement had reached 20 mm, a
306 small horizontal crack approximately 1 mm wide was seen on the S3 support along a
307 line of brick joints. At 35 mm settlement this same crack was 3 mm wide and had gone
308 from one side of the vault to the other (Figure 10-c).

-a

-b

-c

Figure 10. Cracks close to supports S1 (-a), S2 (-b) and S3 (-c).

309

310 The variation in the S4 reaction became stable after 20 mm settlement and no cracks or
311 breaks were observed close to this support. The long gauge sensors fitted to the lower
312 face of the vault close to the elliptical arch S1-S3 (LVDT1, FOS1, LVDT2, LVDT3,
313 LVDT4) recorded maximum displacements of around 0.05 mm (Figure 9-a), but these
314 did not cause any cracks in the area covered by these sensors. However, sensor LVDT5
315 recorded maximum displacements of around 0.9 mm. Figure 10-a shows the crack
316 recorded by this sensor, which started in the arch and propagated horizontally until
317 reaching the S1-S3 arch, where it joined up with a smaller crack. Its evolution was seen
318 to vary at 20 mm settlement, which appears to indicate the beginning of the opening of
319 the crack. The displacements recorded by the sensors fitted to the vault's upper face
320 were somewhat larger, with a bigger opening of the crack on elliptical arch S2-S4.
321 Sensors LVDT6 and LVDT7 placed symmetrically on arch S1-S3 showed very similar
322 behaviour. After a settlement of between 5 and 10 mm (Figure 9-b) the slope of the
323 displacement curves was seen to vary, indicating the appearance of cracks. Sensor FOS3

recorded the opening of a crack at around 15 mm settlement. Cracks also appeared close to sensors FOS2 and LVDT6 and propagated towards support S4 as settlement progressed.

5.3. Structural behaviour

The structural behaviour of the vault suggests that the reactions varied in proportion to the settlement of the support S1 up to the activation of a failure mechanism. From then on, after about 15-20 mm settlement, all four reactions stayed almost constant. Indeed, at this settlement, the crack along the S2-S4 elliptic arch had run almost the complete length of the arch as far as the S2 and S4 supports (Figure 11). At the same time, the LVDT6, LVDT7, FOS2 and FOS3 sensors placed on top of the vault were showing cracks open to between 0.7 and 1.00 mm, indicating much higher tensile stresses than those found in the previously studied specimens. From this point onwards, the vault behaved as two relatively independent structures and the loads were no longer re-distributed around it. This indicated that after this level of settlement the crack continued to widen but did not affect the rest of the structure. At the end of the test, it had reached the underside of the webbing and was 2.5 mm wide.

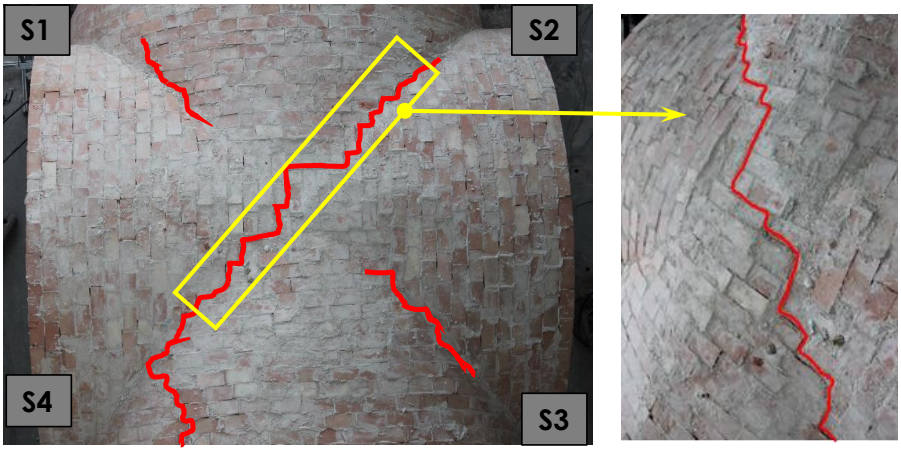

Figure 11. Cracks on the keystone of the vault on elliptical arches S2-S4.

6. Conclusions

This paper describes the experimental results of testing a full-scale timbrel cross vault against the vertical settlement of one of its supports. The main conclusions drawn from the experiment are the following:

- The maximum settlement applied to support S1 was 40 mm, when serious cracking made it advisable to stop the test.
- When settlement was applied to S1, the reactions of S2 and S4 increased by 27 and 50%, respectively, while those of S1 and S3 decreased by 28 and 55%, respectively.
- The vault's structural behaviour indicated that the reactions varied in proportion to the settlement of S1 (up to 5 mm). After 10-15 mm this relationship came to an end, when cracks appeared close to the supports. When the settlement exceeded 15-20 mm all four reactions remained practically constant.
- The most serious cracks in the supports were in S1 (tensile crack), S2 (bending crack) and S3 (tensile crack). Those in S1 and S3 followed the line of brick joints while those in S2 fractured the bricks and were more serious on the outer vault face.
- The largest crack was found on the upper face of the vault and ran from support S2 along the elliptical arch to support S4. Other smaller cracks were found on the arch joining S1 and S3.
- At a settlement of between 15-20 mm, a crack almost joined both sides of the arch between S2 and S4, after which the vault was divided into two relatively independent structures and the re-distribution of loads throughout the vault came to a halt almost completely. This meant that after this point the crack continued to widen but without repercussions on the rest of the structure. This crack also

opened up on the underside of the webbing and by the end of the test had reached a width of approximately 2.5 mm.

Acknowledgements

The authors wish to express their gratitude to the Spanish Ministry of Economy, Industry and Competitiveness for the funding provided through Project BIA 2014-59036-R, and also to *LIC-Levantina Ingeniería y Construcción* and *Grupo Puma* for their invaluable assistance.

References

[1] Abdou L, Saada RA, Meftah F, Mebarki A. Experimental investigations of the joint-mortar behaviour 2006;33:370–84. doi:10.1016/j.mechrescom.2005.02.026.

[2] López-patiño G, Adam JM, Verdejo P, Milani G. Causes of damage to industrial brick masonry chimneys. Eng Fail Anal 2017;74:188–201. doi:10.1016/j.engfailanal.2017.01.014.

[3] Milani G, Valente M. Failure analysis of seven masonry churches severely damaged during the 2012 Emilia-Romagna (Italy) earthquake: Non-linear dynamic analyses vs conventional static approaches. Eng Fail Anal 2015;54. doi:10.1016/j.engfailanal.2015.03.016.

[4] Acito M, Bocciarelli M, Chesi C, Milani G. Collapse of the clock tower in Finale Emilia after the May 2012 Emilia Romagna earthquake sequence: Numerical insight. Eng Struct 2014;72. doi:10.1016/j.engstruct.2014.04.026.

[5] Krentowski J, Chyzy T, Dunaj P. Sudden collapse of a 19th-century masonry structure during its renovation process. Eng Fail Anal 2017;82:540–53. doi:10.1016/j.engfailanal.2017.04.010.

[6] D'Altri AM, Castellazzi G, de Miranda S, Tralli A. Seismic-induced damage in historical masonry vaults: A case-study in the 2012 Emilia earthquake-stricken area. J Build Eng 2017;13:224–43. doi:10.1016/j.jobe.2017.08.005.

[7] Hofer L, Zampieri P, Angelo M, Faleschini F, Pellegrino C. Seismic damage survey and empirical fragility curves for churches after the August 24 , 2016 Central Italy earthquake. Soil Dyn Earthq Eng 2018;111:98–109. doi:10.1016/j.soildyn.2018.02.013.

[8] National Civil Protection Service. Manuale per la compilazione della scheda per il rilievo del danno ai beni culturali, chiese - MODELLO A-DC. Ed. by Simona Papa and Giacomo Di Pasquale; 2013. n.d.

[9] F. Doglioni, A. Moretti, V. Petrini V. Le chiese e il terremoto. Dalla vulnerabilità constatata nel terremoto del Friuli al miglioramento antisismico nel restauro. Verso una politica di prevenzione. Trieste: Lint Editoriale Associati; 1994. n.d.

[10] Regione Toscana. Istruzioni tecniche per l'interpretazione ed il rilievo permacroelementi del danno e della vulnerabilità sismica delle chiese. Venzone: ARX s.c.r.l.; 2003. n.d.

[11] Theodossopoulos D, Sinha B. Structural safety and failure modes in Gothic

406 vaulting systems. … Int Semin Struct … 2008:2–9.

407 [12] Atamturktur S, Bornn L, Hemez F. Vibration characteristics of vaulted masonry
408 monuments undergoing differential support settlement. Eng Struct
409 2011;33:2472–84. doi:10.1016/j.engstruct.2011.04.020.

410 [13] Acikgoz S, Soga K, Woodhams J. Evaluation of the response of a vaulted
411 masonry structure to differential settlements using point cloud data and limit
412 analyses. Constr Build Mater 2017;150:916–31.
413 doi:10.1016/j.conbuildmat.2017.05.075.

414 [14] Carfagnini C, Baraccani S, Silvestri S, Theodossopoulos D. The effects of in-
415 plane shear displacements at the springings of Gothic cross vaults. Constr Build
416 Mater 2018;186:219–32. doi:10.1016/j.conbuildmat.2018.07.055.

417 [15] Foraboschi P. Specific structural mechanics that underpinned the construction of
418 Venice and dictated Venetian architecture. Eng Fail Anal 2017;78:169–95.
419 doi:10.1016/j.engfailanal.2017.03.004.

420 [16] G. Cardani, D. Coronelli, G. Angjeliu. Damage observation and settlement
421 mechanisms in the naves of the Cathedral of Milan. In: Proc. of 10th Int. Conf.
422 on Structural Analysis of Historical Constructions (SAHC 2016), 13–15
423 September 2016, Leuven, Belgium. n.d.

424 [17] C. Valore, M. Ziccarelli. The preservation of Agrigento Cathedral. In: Proc of the
425 18th Int. Conf. on Soil Mechanics and Geotechnical Engineering, 2–6 2013,
426 Paris. p. 3141–44. n.d.

427 [18] Zucchini A, Lourenc PB. A coupled homogenisation – damage model for
428 masonry cracking 2004;82:917–29. doi:10.1016/j.compstruc.2004.02.020.

429 [19] Lourenço PB, Rots J. A multi-surface interface model for the analysis of masonry
430 structures, J. Eng. Mech. ASCE, 1997; 123(7): 660-668. n.d.

431 [20] Milani G, Simoni M, Tralli A. Advanced numerical models for the analysis of
432 masonry cross vaults: A case-study in italy. Eng Struct 2014;76:339–58.
433 doi:10.1016/j.engstruct.2014.07.018.

434 [21] Lorenzis L De, Dimitri R, Tegola A La. Reduction of the lateral thrust of
435 masonry arches and vaults with FRP composites 2007;21:1415–30.
436 doi:10.1016/j.conbuildmat.2006.07.009.

437 [22] Theodossopoulos D, Sinha BP, Usmani AS, Macdonald AJ. Assessment of the
438 structural response of masonry cross vaults. Strain 2002;38:119–27.
439 doi:10.1046/j.0039-2103.2002.00021.x.

440 [23] de Mazarredo Aznar L. Análisis constructivo y estructural de la iglesia de San
441 Juan del Hospital de Valencia, Universitat Politècnica de València 2015. n.d.

442 [24] B. Sáez Riquelme. Iglesias Salón Valencianas del S. XVIII. Levantamiento
443 gráfico, análisis geométrico y constructivo, patología común. PhD Thesis.
444 Departamento de Sistemas Industriales y Diseño. Universitat Jaume I, Castellón
445 (Spain), 2013. n.d.

446 [25] Grupo Puma. www.grupopuma.com. Accesed on 11th April, 2018. n.d.

447 [26] En NE, Une-en N. UNE EN 196-1: 2005. Methods of testing cement. Part 1:
448 Determination of strength. 2005.

449 [27] Lusas 2010 Lusas Reference Manual (Surrey, UK: Lusas). n.d.

[28] Torres B, Payá-Zaforteza Ignacio I, Calderón PA, Adam JM. Analysis of the strain transfer in a new FBG sensor for Structural Health Monitoring. Eng Struct 2011;33:539–48. doi:10.1016/j.engstruct.2010.11.012.

[29] Glisic B, Inaudi D. Fibre optic methods for structural health monitoring. John Wiley & Sons 2008. n.d.

[30] https://www.hbm.com/es/2290/software-adquisicion-de-datos-catman/. Accesed on 11th April, 2018. n.d.

[31] http://www.micronoptics.com/products/sensing-solutions/software/. Accesed on 11th April, 2018. n.d.